Cement & Concrete Composites 37 (2013) 95–107

Contents lists available at SciVerse ScienceDirect

Cement & Concrete Composites

journal homepage: www.elsevier.com/locate/cemconcomp

# Impact of metakaolin characteristics on the rheological properties of mortar in the fresh state

F. Cassagnabère [a,b,c,*], P. Diederich [b], M. Mouret [b], G. Escadeillas [b], M. Lachemi [a]

[a] Ryerson University, Department of Civil Engineering, 350 Victoria Street, Toronto, Ontario, Canada M5B 2K3
[b] Université de Toulouse, UPS, INSA, LMDC (Laboratoire Matériaux et Durabilité des Constructions),135, Avenue de Rangueil, F-31 077 Toulouse Cedex 04, France
[c] SEAC-gf, 47 Boulevard de Suisse 31 021 Toulouse, France

ARTICLE INFO

*Article history:*
Received 7 April 2011
Received in revised form 23 August 2012
Accepted 6 December 2012
Available online 12 December 2012

*Keywords:*
Metakaolin
Morphology
Size distribution
Water demand
Mortar
Slump
Apparent viscosity

ABSTRACT

This study investigated the flow properties (slump, flow time, apparent viscosity at different shear rates) of cement/metakaolin-based mortars. The mix proportion that was used per weight was 3:1:0.5 (sand:-binder:water), and the binder was composed of either 100% cement (OPC) or combinations of cement and metakaolins (MKi). Replacement rates of cement with MK were 12.5% and 25% per weight. Four metakaolins produced in two areas with two processes of calcination (fluidized bed and flash calcination) were employed. Their chemical and mineralogical compositions, physical properties, size distribution and morphology were fully characterized. Relationships between various MK properties and the flow properties of mortars were studied. Results show that metakaolins can produce significant differences in the flow of mortars, depending on their physical and chemical properties. In particular, the nature and content of impurities are key factors acting directly on the morphology of the distribution of the constituting particles and the water demand of MK. All these parameters control the rheological properties of the resulting cementitious suspensions. The mode of calcination is a second order factor influencing the shape of particles, since the flash process can smooth the surface of the smallest particles. More specifically, the high quartz content present in flash MK as rounded particles is minimally or not at all affected by the calcination process, and maintains flow properties more successfully than mortar incorporating cement only.



## 1. Introduction

With a current global cement production rate of 1.2 billion tons per year that is projected to grow to 3.5 billion by 2015 [1] the ever-growing demand is becoming an increasing financial burden for governments and municipalities. Also, the use of OPC (for instance, CEMI 52.5R in European standard) poses environmental concerns (significant $CO_2$ emissions [2] and significant thermal energy [3]) and incurs increased costs due to eco-taxes established following the Kyoto Protocol [4].

The search for alternative binders and/or cement replacement has led to the use locally available mineral additions. At present, metakaolins, as pozzolanic materials, appear to satisfy a number of economical, performantial and environmental requirements.

Metakaolin (MK), $Al_2Si_2O_7$ or $AS_2$ in cementitious notation, is obtained through the calcination of kaolinitic clay (Fig. 1, according to [5]) at temperatures between 700 °C and 800 °C. The dehydroxilization is brought on by the application of heat over a defined period of time. Two types of calcination exist:

(i) "Flash process," in which, after a crushing phase, the clay particle is immediately calcined as it goes through the flame burner [6–8];
(ii) "Fluidized bed process," in which the raw clay is baked in a kiln over several hours before the crushing phase [9,10].

Compared to cement production, the production of MK leads to less $CO_2$ (Eq. (1)) being released into the atmosphere (1 ton of MK produced = 175 kg of $CO_2$ released [11]). It also requires less thermal energy than that consumed during clinker production (1 ton of MK produced = 2.95 GJ).

$$Al_2O_3(SiO_2)_2(H_2O)_2 \rightarrow Al_2O_3(SiO_2)_2(H_2O)(H_2O)x + (2-x)H_2O \quad (1)$$

The pozzolanic activity of metakaolin (MK) in cement-based materials in the hardened state has been widely studied in terms

* Corresponding author at: Université de Toulouse, UPS, INSA, LMDC (Laboratoire Matériaux et Durabilité des Constructions), 135, Avenue de Rangueil, F-31 077 Toulouse Cedex 04, France. Tel.: +33 5 61 55 67 11; fax: +33 5 61 55 99 49.
*E-mail addresses:* franck.cassagnabere@insa-toulouse.fr (F. Cassagnabère), paco.diederich@insa-toulouse.fr (P. Diederich), michel.mouret@insa-toulouse.fr (M. Mouret), gilles.escadeillas@insa-toulouse.fr (G. Escadeillas), mlachemi@ryerson.ca (M. Lachemi).

0958-9465/$ - see front matter © 2012 Elsevier Ltd. All rights reserved.
http://dx.doi.org/10.1016/j.cemconcomp.2012.12.001

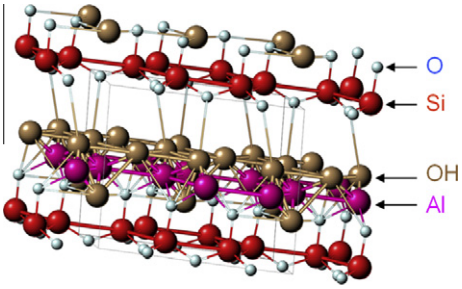


**Fig. 1.** Kaolinite structure [5].

of neoformed hydrated phases (C–S–H gel, $C_2ASH_8$, $C_4AH_{13}$ and $C_3AH_6$) [12–14], and improvement of hardened properties (strength, durability) for replacement rates ranging from 10% to 25% by mass of cement. [15–18]. However, despite the fact that there are numerous studies dealing with hardened properties of MK-based cementitious materials, studying the impact of MK incorporation on properties of cementitious materials in the fresh state is important to ensure good placing conditions. Many studies have also been conducted on this subject.

Gaboriau et al. [19] showed that the major problem with metakaolin (MK produced by fluidized bed) incorporation into cementitious material is the water requirement, which is due to a high specific area (17 $m^2/g$) and an involved morphological structure (irregular structure).

Wild et al. [20] studied the workability of concretes incorporating metakaolin (MK produced by fluidized bed with 40% impurity) at replacement levels by mass of ordinary Portland cement (OPC) at 0%, 5%, 10%, 15%, 20%, 25%, and 30%, with a constant the water-binder ratio (w/b) (0.45). OPC concrete mixture proportion was 1:2.3:3.4 (water:binder:aggregates). The results showed that the increased incorporation of superplasticizer (from 0% to 3.6% of binder weight), to offset the increased water demand at increased metakaolin levels (0–30%), increased the slump (5–90 mm). An increase in compacting factor (0.81–0.90) and a decrease in Vebe-time (26–5 s) occurred when MK was incorporated up to 30%.

Brooks and Johari [16] reported on the slump and setting times of concretes containing 0%, 5%, 10%, and 15% metakaolin (MK produced by fluidized bed with 20% impurity). The control concrete mixture proportion was 1:1.5:2.5, with water-binder ratio by mass (w/b) of 0.28. A decrease in slump (100–5 mm) occurred with the increase in MK content (0–15%).

Bai et al. [21] used a neural network to predict the workability of concrete incorporating metakaolin (MK produced by fluidized bed with 20% impurity). On the basis of developed models, the effects of MK were analyzed on iso-slump maps as a function of w/b (0.25, 0.4, 0.5) and cement/MK combinations. The prediction reflected the effect of the graduated decrease in slump with pozzolanic replacement of Portland cement up to 15% MK.

Li and Ding [22] investigated the consistency of Portland cement containing metakaolin (MK produced by fluidized bed with 25% impurity), comparing pastes containing 100%, and 90% cement and 10% MK, respectively. For the reference binder, the standard consistency was 29.1% [23]. The cement-only mixture had the lowest water requirement, and the MK-blended cement had the highest water requirement at 29.1%.

Badogiannis et al. [24] reported the results of water demand and setting times of cements containing five metakaolins. The metakaolinite contents of the first four metakaolins (MK1, MK2, MK3, and MK4, derived from poor Greek kaolins) were 36%, 37%, 71%, and 49%, respectively, whereas in the final, high-purity commercial metakaolin (MKC), the contents were 95%. Cement was replaced with 0, 10, and 20% metakaolin by mass. The study concluded that blended cements require significantly more water than the relatively pure cement. Metakaolin content of 10% resulted in a water demand that varied from 29.0% to 32.5%, while the PC was 27.5%. Metakaolin content of 20% resulted in a water demand that varied from 31.5% to 41.5%. MK1 and MK2 showed the best behavior, with a lower increase in water demand that could be attributed to the high fineness of the metakaolin and to particle size distribution with more small particles.

These studies point out a number of relevant parameters for the influence of MK on the properties of fresh cement-based mixes, including water demand, purity and particle size. However, several questions remain to be studied: (i) is it possible to categorize MK in relation to the flow properties of the whole mix, just based on the criterion of MK water demand, and (ii) can an MK with a significant water requirement and dilution generated by impurity (quartz or illite) be incorporated into cementitious materials without alteration of behavior in the fresh state?

This paper is part of a broader study dealing with the replacement of cement with metakaolin in slip-forming concrete for manufacturing precast and steam-cured elements. Here, four metakaolins that differed in terms of the calcination process, impurity content and water demand were examined. These properties, coupled with investigations on particle morphology, were considered in order to assess the influence of MK incorporation on the rheological properties and workability of fresh mortars.

## 2. Experimental program

### 2.1. Raw materials

#### 2.1.1. Cement

A Portland cement CEM I 52.5R, which complied with the European standard EN 197-1 [25], was used. The denominations "R" and "52.5" correspond to a high reactivity at early ages, and a 28-day minimum compressive strength of 52.5 MPa guaranteed on normalized mortars according to EN 196-1 [26], respectively. All characteristics (physical and chemical) are given in Table 1. The size distribution of the cement is plotted on Fig. 2.

#### 2.1.2. Normalized sand

The normalized sand (Leucate) was uncrushed, siliceous (98% in weight), natural sand ranging from 0.08 mm to 2 mm. Grading

**Table 1**
Physical and chemical properties of CEM I 52.5R cement.

| | |
|---|---|
| *Physical characteristics* | |
| Specific gravity ($g/cm^3$) | 3.15 |
| Fineness by ($cm^2/g$) | |
| – Blaine method: | 4200 |
| – BET $N_2$ method: | 13,000 |
| $D_{50}$ (μm) | 13.00 |
| Coefficient of uniformity Cu** | 4.3 |
| Coefficient of curvature Cc*** | 1.2 |
| Water demand [27] | 0.28 |
| Compressive strength at 28 days (MPa) | 64.70 |

*Chemical composition**

| $SiO_2$ | $Al_2O_3$ | $Fe_2O_3$ | CaO | MgO | $K_2O$ | $NaO_2$ | $SO_3$ | LOI |
|---|---|---|---|---|---|---|---|---|
| 19.85 | 4.80 | 2.75 | 63.60 | 1.45 | 0.90 | 0.15 | 3.45 | 2.20 |

*Composition and Bogue formula**

| Clinker | Mineral admixture | Gypsum | $C_3S$ | $C_2S$ | $C_3A$ | $C_4AF$ |
|---|---|---|---|---|---|---|
| 92.00 | 3.00 (limestone) | 5.00 | 62.00 | 10.20 | 8.10 | 8.40 |

* %Weight.
** $Cu = D_{60}/D_{10}$ where $D_{10}$ and $D_{60}$ are the particle diameters at 10% and 60% passing.
*** $Cc = D_{30}^2/D_{10}D_{60}$ where $D_{10}$. $D_{30}$ and $D_{60}$ are the particle diameters at 10%. 30% and 60% passing respectively.

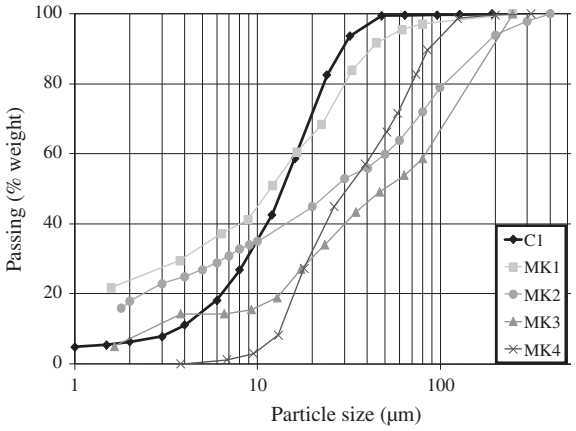


**Fig. 2.** Mass size distribution of cement and MKi (sedigraphy method).

complied with the requirements of EN 196-1 [26]. The absorption value of the sand was 0.19%, and the relative density at saturated dry surface condition was 2.68.

### 2.1.3. Metakaolins (MKi)

Four metakaolins (MK1–MK4) from two extraction areas, calcined with two different processes (fluidized bed and flash), were studied. The first production area corresponds to a highly pure deposit. Metakaolins from the second area have a higher impurity rate, particularly pertaining to quartz. Table 2 presents information about MK production (extraction area and calcination mode). The physical, chemical properties and molar proportion of the mineralogical phase of metakaolins, which also appear in Table 2, are covered in more detail in Section 3.1. The size distribution of the four MK is shown in Fig. 2.

## 2.2. Binder and mixing

The batch for the reference mix without MK, designed according to European standard EN 196-1 [26], was composed of three parts by mass of sand, one part of cement and a half part of water. All mixes with MK had the same proportions of sand, powder (cement and mineral admixture) and water as the reference mix. As it generally used in the concrete industry [27], cement replacement with MK was expressed as the mass fraction of cement in the control mix. Replacement rates were 12.5% and 25%. Beyond 25% replacement, preliminary studies showed that workability and placing of mortars were impaired due to water demand of MK [28]. Table 3 shows the denominations and compositions used in this study. For each composition, a 1.2L batch was prepared using a mixer with 2L capacity. The mixing sequence complied with EN 196-1 [26].

## 2.3. Tests

### 2.3.1. Powder characterization

Based on information obtained from XRD, SEM, chemical composition and fineness, characterization of size distribution and morphology were carried out to explain the flow properties of MK-based mortars, depending on the nature of MK. The flow properties of suspensions were largely dependent on the size and shape of the suspended particles, which is illustrated in Legrand and Metzner [29,30]. To assess differences in the flow behavior of the studied mortars, particle size and shape information of cement and metakaolin were determined using an optical microscope equipped with an automated particle characterization system. For each powder analyzed, the measurement procedure was composed of two steps.

**Table 2**
Metakaolins (MKi) used within the test program.

| | Production area A (Clérac, 17 France) | | Production area B (Fumel, 47 France) | |
|---|---|---|---|---|
| *Production areas* | | | | |
| Calcination by fluidized bed | MK1 | | MK3 | |
| "Flash" calcination | MK2 | | MK4 | |
| | MK1 | MK2 | MK3 | MK4 |
| *Physical properties* | | | | |
| Specific gravity (kg/m$^3$) | 2519 | 2500 | 2608 | 2600 |
| BET $N_2$ (cm$^2$/g) | 187,000 | 180,000 | 120,000 | 150,000 |
| $D_{50}$ (μm) | 11.50 | 26.00 | 50.00 | 31.00 |
| Cu | 42.5* | 50.0* | 32.8 | 3.2 |
| Cc | 2.35* | 0.98* | 2.58 | 0.73 |
| Water demand [27] | 0.62 | 0.72 | 0.59 | 0.57 |
| Strength activity index | 1.06 | 1.03 | 0.94 | 0.99 |
| | MK1, MK2 | | MK3, MK4 | |
| *Chemical composition (%weight)* | | | | |
| $SiO_2$ | 56.20 | | 68.70 | |
| $Al_2O_3$ | 37.20 | | 25.70 | |
| $Fe_2O_3$ | 1.40 | | 2.30 | |
| CaO | 1.20 | | 0.70 | |
| MgO | 0.20 | | Trace | |
| $K_2O$ | 1.20 | | 0.20 | |
| LOI | 2.10 | | 0.80 | |
| | MK1, MK2 | | MK3, MK4 | |
| *Molar proportion of mineralogical phase and associated structural formulas (%)* | | | | |
| Metakaolin $Al_2O_3(SiO_2)_2$ | 68 | | 53 | |
| Quartz $SiO_2$ | 13 | | 43 | |
| Illite $K_{0.90}(Si_{3.30}\ Al_{0.70})\ (Al_{1.80}\ Fe_{0.05}\ Mg_{0.15})\ O_{10}\ (OH)_2$ | 11 | | Trace | |
| Haematite $Fe_2O_3$ | Trace | | 1 | |
| Water $H_2O$ | 5 | | 1 | |
| Other | 2 | | 1 | |

* Values deduced from the estimate of $D_{10}$ values (0.4 μm and 1 μm for MK1 and MK2, respectively) on laser diffraction curves.

**Table 3**
Mix designs of one batch of mortar (g).

| Designation ($i$ = 1. 4) | Cement | Metakaolin MKi ($i$ = 1.4) | Sand | Water |
|---|---|---|---|---|
| M-0% | 450.00 | 0.00 | 1350.00 | 225.00 |
| M-12.5MKi | 393.75 | 56.25 | 1350.00 | 225.00 |
| M-25%MKi | 337.50 | 112.50 | 1350.00 | 225.00 |

(i) The powder was dispersed with an instantaneous pulse of compressed air; after several trials, the applied pressure values of four bars and two bars for metakaolins and cement, respectively, were chosen as a compromise between a homogeneous dispersion and a random orientation in each analyzed frame and a limitation of touching particles. In the case of metakaolin, it was not always possible to ensure that particles did not physically touch.

(ii) Several areas of the sample were observed at a magnification of 20×; particle size and shape indicators were determined on 30,000 grains (since the measured properties did not significantly change from 15,000 particles). 20× magnification was chosen to avoid particles that were larger than 40% of the field of view, as recommended, and provide sufficient resolution for particles larger than 1 μm. Accordingly, size and shape analysis was not conducted on the smallest grains.

From each particle included in the sample, a two dimensional (2D) image was captured and various size and shape parameters

were calculated. A hole filling was applied to each image for an accurate estimation of particle length and width. The size was evaluated using the Circle Equivalent diameter (CE diameter), which is the diameter of a circle with the same area as the 2D image of the particle. A number distribution in terms of size could then be deduced.

A single shape indicator cannot completely discriminate different particle shapes [31]. However, based on analysis of projected particle images issued from observations using a light microscope equipped with a digital camera, Hentschel and Page [32] found that at least two descriptors are required to characterize the attributes of shape, i.e., elongation and ruggedness. Accordingly, shape was described in this study using three 2D descriptors ranging from 0 to 1, and defined as the ratio of two particle size measurements.

*Circularity* is the ratio of the perimeter of a circle with the same area as the particle divided by the perimeter of the actual particle image. Circularity quantifies how close the shape is to a perfect circle and is sensitive to both overall shape and surface roughness.

*Convexity* is the ratio between the convex hull perimeter and the actual particle perimeter. Convexity is sensitive to changes in the surface roughness of a particle, but not its overall shape. A value of 1 corresponds to a smooth shape while a value closer to 0 is representative of a very "spiky" or irregular object.

*Elongation* is calculated as 1-width/length. A shape that is symmetrical in all axes such as a circle or square, has an elongation value of 0; shapes with large aspect ratios have an elongation closer to 1. Elongation is unaffected by surface roughness.

#### 2.3.2. Fresh test characterization

Immediately after mixing, mortars were subjected to workability tests (Sections a and b) and rheological tests (Section c).

(a) Static test

The slump test was used to determine static properties of fresh mortars at 5, 15, 30, 45, 60 min after $t_0$ (water introduction in drying blending). The slump was measured using a mini-cone (Fig. 3a) with dimensions proportional to the Abrams cone, with a ratio of 0.5 [33].

(b) Dynamic test

The dynamic test was performed with an LCL workabilimeter [34]. The experimental instrument, shown in Fig. 3b, recorded the flow time of vibrated mortars placed in a metallic container. This test conveyed exclusively viscous flow ability because the yield stress was inhibited by vibration (50 Hz and 1 m s$^{-2}$). Measurements were also carried out at 5, 15, 30, 45, 60 min after $t_0$ (water introduction in the dry blend).

(c) Rheological test

A modified viscometer Rotovisco RV2 (Haake) was used for rheological testing. To avoid slip, the inner rotating bob was replaced with a six-blade vane (Fig. 3c), which drags a cylindrical block of mortar. The gap was wide enough to allow the medium to be considered infinite. Each test performed at 20 °C required 1 L of mortar. All the mortars were subjected to vibration because they exhibited a stiff consistency. To that end, the outer cup was fixed on a vibrating table (50 Hz and 1 m s$^{-2}$) and the elimination of the time-dependent behavior by the vibration enabled a single significant flow curve, obtained by decreasing velocities [29]. The same experimental protocol was used for all mortars to obtain the same shearing history, so that it took place during the first 15 min after mixing. The directions for use and the equations for shear stress $\tau$ and velocity gradient $\dot{\gamma}$ have been previously published [29].

## 3. Results

### 3.1. Powders characterization: C and MKi

Before developing the properties of mortars in the fresh state, the characterization of the powders were considered in more detail.

#### 3.1.1. Chemical composition and mineralogical characteristics of MK

As far as chemical properties are concerned (Table 2), the fundamental difference between the MKi coming from the two production areas is the ratio of $SiO_2/Al_2O_3$ rate (1.51 for area A and 2.67 for area B). Considering a ratio of $SiO_2/Al_2O_3$ equal to 1.18 in pure MK, it can be assumed that the impurity content of MK1 and MK2 (area A) is less than MK3 and MK4 (area B).

For mineralogical characteristics (Table 2), XRD analysis allows us to compare rate of amorphization semi-quantitatively, as obtained by the area of halo centered on 3.8 Å ($2\theta = 27.07°$). As shown in Fig. 4a, a more amorphous structure was visible for metakaolins created by flash process (MK2 and MK4) than those created by fluidized bed (MK1 and MK3). Moreover, other crystallized phases – which are considered impurities – were also in the four MKi. But, as expected, more impurities (quartz, illite and kaolinite) were present in MK3 and MK4 (area B) than in MK1 and MK2 (area A). Using structural formulas (Table 2), it was found that the metakaolinite content was more important for MKi coming from site A (≈68%) than for the MKi from site B (≈53%).

#### 3.1.2. SEM observation of MK powder

Fig. 5 presents SEM observation in secondary electron imaging mode. Qualitative comments are outlined below.

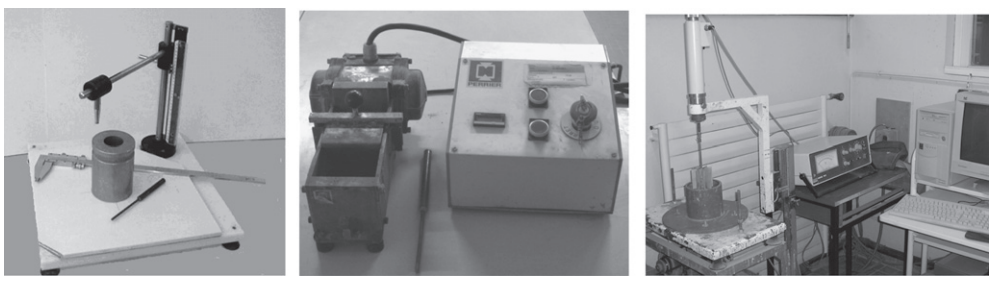

(a) Mini-cone slump (b) LCL workabilimeter (c)Viscosimeter

**Fig. 3.** Fresh material tests.

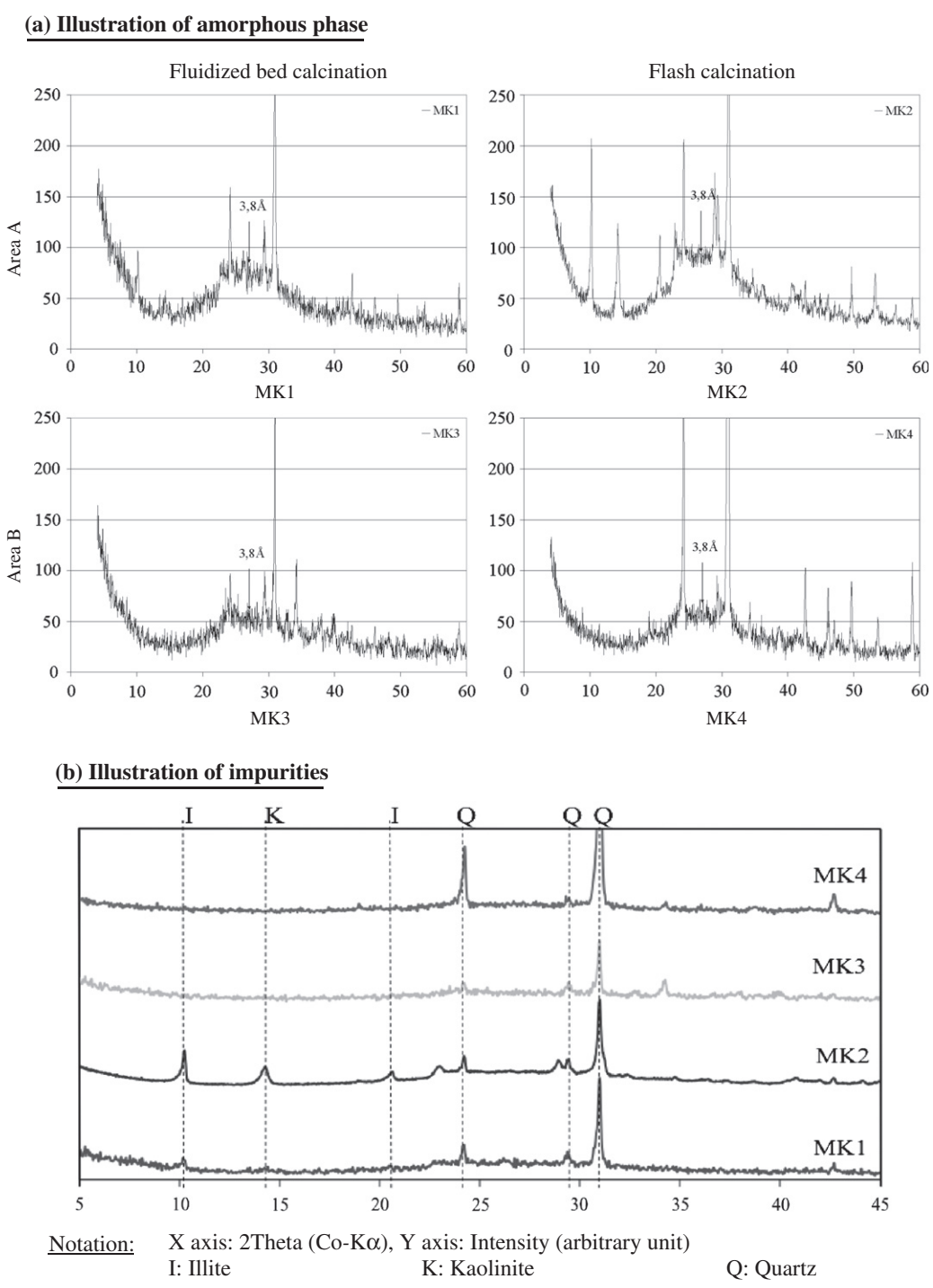


**Fig. 4.** XRD diagrams of $MK_i$.

(a) Particle size

MK1 and, to a lesser extent, MK2 (area A), seemed to incorporate more fine particles. Coarse elements (around 100 μm) were visible in MK3 and MK4 (area B).

(b) Particle morphology

Despite a layer structure that is representative of kaolinite (Fig. 1), two kinds of morphology can be observed according to the calcination process. First, for MK1 and MK3, the sequence of fluidized bed calcination followed by crushing phase generated a particle population with an angular and salient shape. Second, when the process was made up of the crushing phase followed by flash calcination, metakaolin (MK2 and MK4) exhibited more rounded particles. Moreover, the instantaneous thermal treatment might have generated vitrified particles with a perfect roundness.

The observed differences in shape, size, distribution and impurity content of the tested metakaolins should have an influence on the flow properties of mortar at the fresh state. Size distributions and morphology of powders are now developed in a quantitative way. This characterization of metakaolins will be discussed further

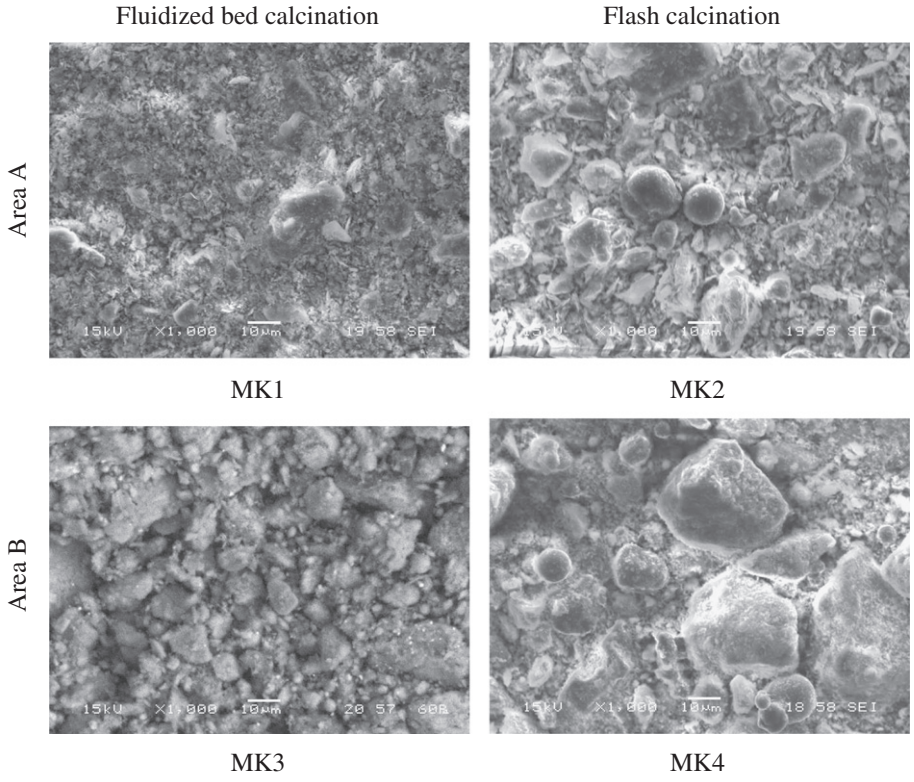


**Fig. 5.** SEM images of $MK_i$ (1000× magnification, SEI mode).

later in this paper, with respect to their origin and mode of production (Section 4.1) and in relation with the flow properties of mortars (Section 4.2).

### 3.1.3. Size distribution and morphology of powders

(a) Mass size distribution

Considering the grading coefficient *Cu* and *Cc* (Tables 1 and 2), fairly narrow particle size distributions with a predominance of fine particles were observed on cement and MK4, while spread particle size distributions with a predominance of fine particles were visible for MK1 and MK2. Only MK3 presented a spread distribution without a predominance of any size class. Fig. 2 presents the grading size distribution of cement and MKi obtained by the sedigraphy method (dispersion of particles by means of ammonia).

When compared with cement, the content of fine particles was larger for MK1 and MK2, and smaller for MK4 (10 μm passing less than 5%). This is consistent with SEM observations. In parallel, MK2 and MK3 exhibited the most extended particle size distribution (Fig. 2). However, the significant amount of coarse particles in MK2, MK3 and, to a lesser extent, MK4 can be attributed to agglomerates of fine particles insufficiently dispersed during sedigraphy measurement. Indeed, the interparticle forces (electrostatic and Van der Waals ones) can be emphasized by the admitted flat-shaped particles of metakaolin [35]. In addition, the significant fineness (>12 $m^2/g$, Table 2) can be attributed to a distribution finer than the measured one, but also to an existing surface porosity and ruggedness of particles. This significant fineness is linked to a high water requirement (Table 2).

(b) Number size distribution

The number size distributions of cement and metakaolins, based on the CE diameter, are shown in Fig. 6. No comparison is possible with the sedigraphy method in Fig. 2 (where a mass or volume distribution is made according to the hydraulic diameter), but supplementary information is available. Indeed, based on evidence shown in Fig. 6, the number of particles was more important for MK4 than for the other metakaolins in the [1–10[-μm class. Below 1 μm, similar distributions were observed for metakaolins (a difference which is at most equal to 3% passing). In comparison

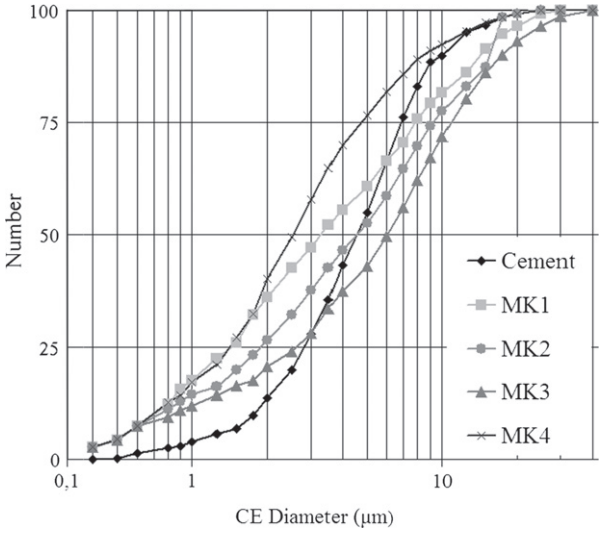


| | Cement | MK1 | MK2 | MK3 | MK4 |
|---|---|---|---|---|---|
| D(n, 10) μm | 1.7 | 0.7 | 0.8 | 0.9 | 0.9 |
| D(n, 50) μm | 4.6 | 3.4 | 4.6 | 6.0 | 2.5 |
| D(n, 90) μm | 9.8 | 13.7 | 15.2 | 16.9 | 8.8 |
| % < 5μm | 55.3 | 60.9 | 52.9 | 43.6 | 76.5 |

**Fig. 6.** Number size distribution of powders (image analysis).

with cement, coarser particles were visible beyond 4 μm, 5 μm, 6 μm and almost 10 μm for MK3, MK2, MK1 and MK4, respectively. This can be attributed to agglomerates, considering how difficult it was to completely avoid the touching of particles in metakaolin powders. This is an issue inherent to the nature of metakaolin, and particularly the flat-shaped particles that metakaolin contains.

(c) Morphology

The mean values per size class of the shape descriptors, i.e., convexity, circularity and elongation, as well as the 95% confidence intervals for the mean values, are plotted in Fig. 7. Normality tests such as the one conducted by Shapiro–Wilk [36] showed that the descriptors are not normally distributed. In that case, the confidence intervals could not be calculated by classical parametric methods. Instead, they were produced using the bootstrap technique [37]. This re-sampling technique consisted of randomly choosing a set of data pertaining to the sample of particles, with replacement among the initial data of the sample. Thus, while a value appears in the actual sample, it may not appear in the re-sample, or could appear more than once. The re-sampling was repeated 1000 times to build a great number of samples, on which 1000 mean values of descriptors were calculated and a distribution of mean values obtained. Finally, a 95% confidence interval was deduced from the 2.5th and 97.5th percentiles of the distribution. Several observations can be made based on Fig. 7.

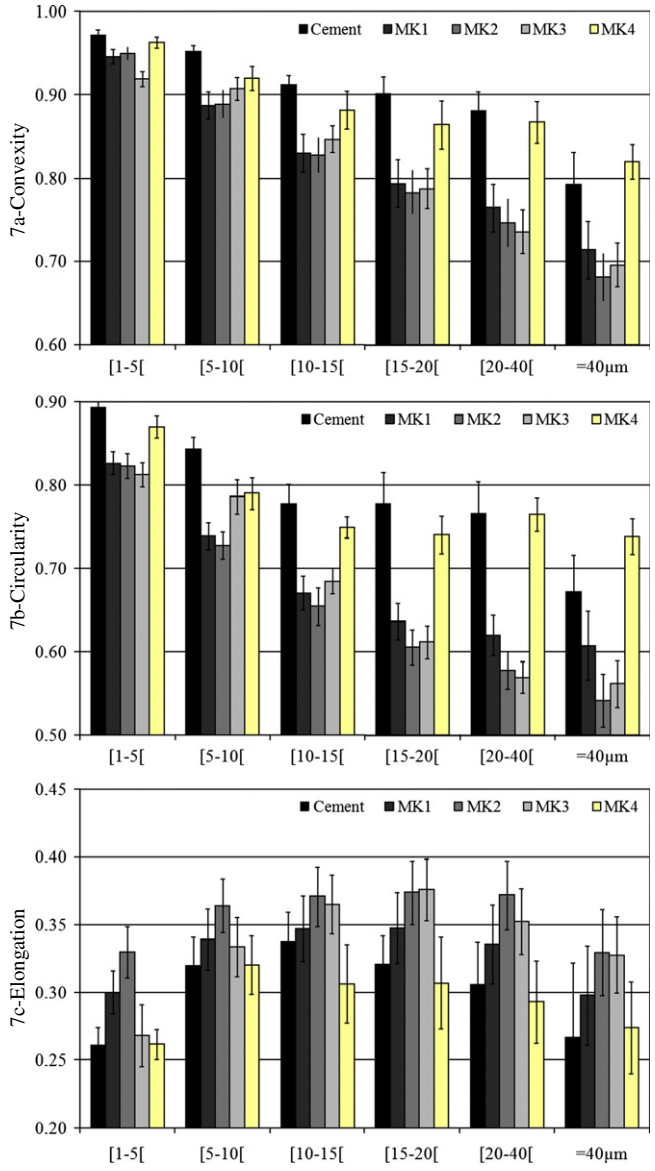


**Fig. 7.** Shape descriptors of powders – convexity (7a), circularity (7b), elongation (7c).

- Similar evolutions were observed according to the nature of the powder for convexity ((Fig. 7a) and circularity (Fig. 7b); the closer a particle is to a circle, the less surface ruggedness it presents and *vice versa*. This finding is consistent with a previous study on particles of metal alloys [32]. Accordingly, both descriptors will also be discussed indirectly in the points below.
- Irrespective of size class, the roundest and the least elongated particles were observed in the cement and MK4. The shape descriptors did not change significantly between the two powders.
- In comparison with MK1, MK2 and MK3, metakaolin MK4 contains significantly fewer elongated particles and more rounded and smoothed particles ranging in size from 10 μm to 40 μm (Figs. 7a and b). In the finest ([1–5[ μm) and coarsest (⩾40 μm) classes, all of these significant differences remained except for elongation. Elongation was significantly higher in the [1–5[-μm class for MK2 than for the other metakaolins.
- In the [5–10[-μm class, circularity and convexity were significantly higher for cement than for all four metakaolins. Elongation remained the highest for MK2.

### 3.2. Flow properties of mortars

This section details a systematic comparison that was carried out between the flow properties of mortars made with two kinds of binder; cement only or a cement and metakaolin combination. As mentioned earlier, all mixes incorporated the same amount of water (Table 3).

#### 3.2.1. Slump

Table 4 shows slump values at different times, after the incorporation of water into the dry mix ($t_0$). When metakaolin was incorporated, there was a decrease in slump. This decrease was emphasized when the replacement rate was increased from 12.5% to 25%, so much so that only slight slump or no slump at all was observed at $t_0$ + 5 min. The dramatic decrease in slump at $t_0$ + 5 min is associated with the increase in the water demand of metakaolin (Table 2). At a replacement rate of 25%, no slump was measured from $t_0$ + 30 min. It is well-known that slump is linked to yield stress (see [38] for an example). Hence, the incorporation of metakaolin should increase yield stress in the resulting suspensions. In fact, the irregular surface texture and the possible high open porosity of metakaolin, globally associated with the BET-specific surface area, decreased the available water around particles and therefore the inter-particle distance. The yield stress can then be accentuated as a continued network of inter-particle

**Table 4**
Slump (mini-cone) according to the time (mm) – experimental dispersion = ±3 mm.

| $t_0$ + ... | ...5 min | ...15 min | ...30 min | ...45 min | ...60 min |
|---|---|---|---|---|---|
| M-0 | 38 | 28 | 9 | 5 | 1 |
| M-12.5MK1 | 12 | 2 | 0 | 0 | 0 |
| M-12.5MK2 | 1 | 0 | 0 | 0 | 0 |
| M-12.5MK3 | 16 | 7 | 2 | 0 | 0 |
| M-12.5MK4 | 11 | 6 | 2 | 0 | 0 |
| M-25MK1 | 0 | 0 | 0 | 0 | 0 |
| M-25MK2 | 0 | 0 | 0 | 0 | 0 |
| M-25MK3 | 3 | 0 | 0 | 0 | 0 |
| M-25MK4 | 5 | 1 | 0 | 0 | 0 |

bonds. The small inter-particle distance can also promote particle bridging due to the development of the first hydration products, which involves an increase of yield stress (decrease in slump) with time.

### 3.2.2. LCL workability

Supplementary information on the flowability of mortars incorporating metakaolin can be obtained by means of the LCL workabilimeter (Fig. 3b). Fig. 8 presents the variation of the measured flow time versus test time. The same behavior was observed between the reference mortar (M-0) and the mortar incorporating MK4, at a replacement rate of 12.5% (M-12.5MK$_i$ in Fig. 8). MK2 and MK3 showed a slight increase in flow time up to 15 min; beyond 15 min, workability loss began to be significant. The longest flow time was consistently observed in the case of mortar incorporating MK1.

At a replacement rate of 25% (M-25MK$_i$ in Fig. 8), loss of workability was visible whatever the nature of metakaolin, in comparison to the reference mortar (M-0) and the M-12.5MKi mortars. This result is consistent with Courard et al. [18]. When MK4 was incorporated, the increase in flow time was slight. Conversely, this increase was very marked when MK1 or MK2 or MK3 were incorporated. In these cases, beyond 30–40 min after water-binder contact, the recommended validity limit of 90 s was exceeded.

### 3.2.3. Apparent viscosity

The variations in slump and flow time can be associated with variations in rheological properties, i.e., static yield stress and viscosity, respectively. Measurement of the static yield stress was not possible because it exceeded the limit capacity of the viscometer for all the mortars. The application of vibration enabled flow, and shear dependent properties were determined in a viscous regime

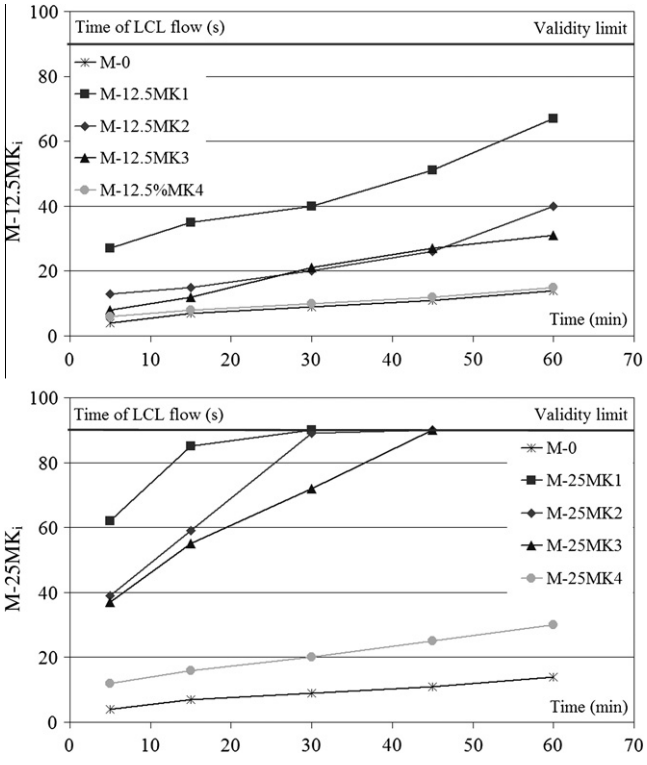


**Fig. 8.** Evolution of time of LCL workability according to the time (M-12.5MK$_i$, M-25MK$_i$).

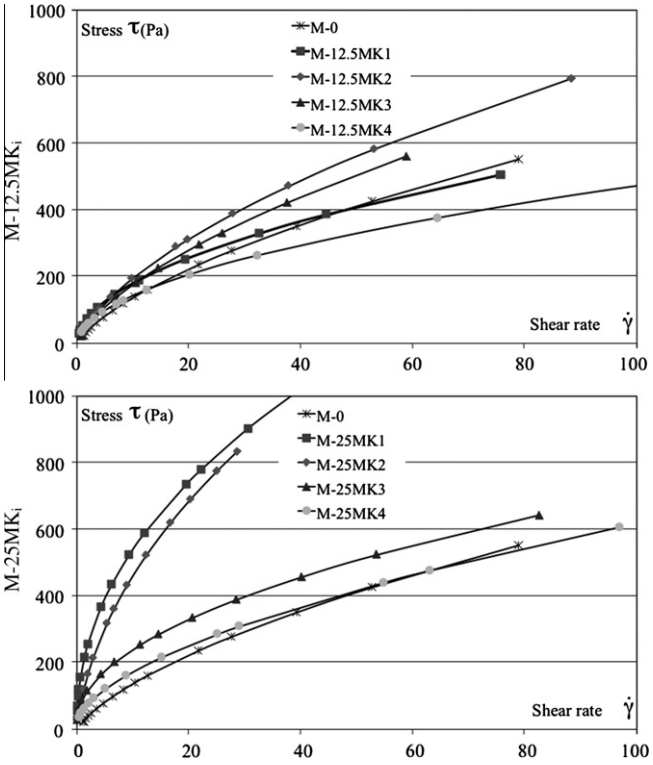


**Fig. 9.** Flow curves for M-0, M-12.5MK$_i$and M-25MK$_i$.

($\tau_0 = 0$ in the Herschel–Bulkley model, $\tau = \tau_0 + m \times \gamma^n$ chosen to describe the flow in Fig. 9).

All the studied mortars exhibited a shear thinning behavior (Fig. 9) typical of the flocculent structure of cement-based suspensions free of (super) plasticizer [29,39]. Even if the rheological behavior was not modified by the incorporation of MK (the rheological behavior index $n$ remains less than 1), there were obvious differences based on the nature and dosage of MK. These differences are discussed here in terms of apparent viscosities that were calculated from flow curves as the ratio between the shear stress and shear rate. Then, for a given shear rate, quotients of the viscosity measured on M-XMK$_i$ mortars were calculated, and divided by the viscosity of reference mortar (M-0). These quotients, or relative viscosities, are shown in Fig. 10. Maximum and minimum relative viscosity values were also plotted in Fig. 10, which accounts for the experimental accuracy on viscosities (5%). Shear rate values of 2, 5, 15 and 25 $s^{-1}$ were chosen because they are representative of the evolution for all common shear rates applied to the mortars. In addition, these values were within the range of typical shear rates encountered in concrete placement [40]: 2 $s^{-1}$ and 5 $s^{-1}$ are related to traditional casting in formwork, whereas 15 $s^{-1}$ and 25 $s^{-1}$ represent a pumping context. Two main observations can be made based on Fig. 10.

- When metakaolin was incorporated, there was most often a significant increase in viscosity, since relative viscosity values were greater than the experimental scatter of the reference mortar; only the M-12.5MK4 mortar exhibited viscosities that were similar to the reference beyond a shear rate value of 2 $s^{-1}$.
- Whatever the shear rate, there was a dramatic increase in viscosity when the amount of metakaolin was increased in mortars incorporating MK1 or MK2. The use of MK3 did not result in as marked an increase as the shear rate value of 15 $s^{-1}$. Conversely, the viscosities of MK4 mortar were not significantly modified from the 12.5% to the 25% replacement level.

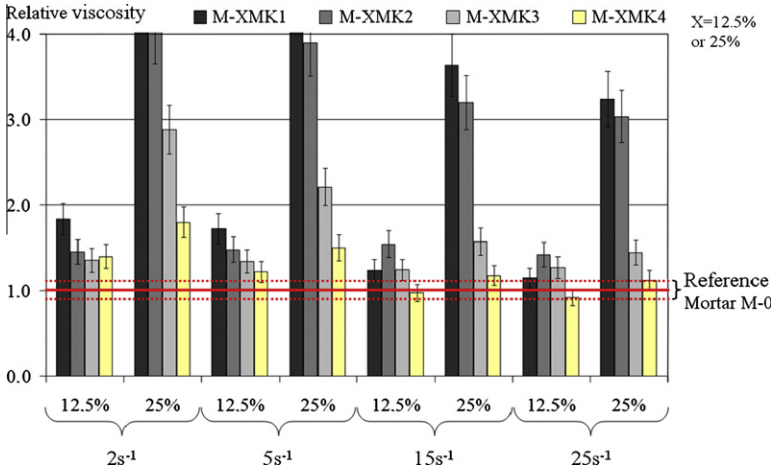


**Fig. 10.** Relative viscosity according to velocity gradient (2, 5, 15 and 25 $s^{-1}$).

## 4. Discussion

A number of obvious differences were visible between shape indicators according to the nature of the metakaolin (Section 3.1). It was also evident that the nature and dosage of MK could modify the flow of the resulting mortars at a constant water content (Section 3.2). There are two objectives in this section: (i) to discuss the possible causes of the change in MK morphology (Section 4.1), (ii) to study the relationships between flow properties of mortars and MK properties (Section 4.2). To achieve these objectives, the existence of relationships between relevant parameters was determined using the Kendall rank "*tau*" correlation coefficient, which was chosen because it is insensitive to an utmost point in the scatter plot and no hypothesis on the normality of variables is needed to calculate it.

The Kendall "*tau*" coefficient calculates the degree of correspondence between two parameters for which paired observations are available. The "*tau*" value is determined by identifying the concordant pairs (a simultaneous increase in the parameters between two observations) and the discordant pairs (in two observations, an increase in one parameter and decrease in the other one) among all possible defined pairs (Eq. (2)) [41].

$$\text{“}tau\text{”} = \frac{\sum concordant\ pairs - \sum discordant\ pairs}{Total\ number\ of\ possible\ pairs} \quad (2)$$

Considering Eq. (2), "*tau*" will take values between −1 and +1, with a positive correlation indicating that the ranks of both variables increase together, while a negative correlation indicates that as the rank of one variable increases, the other one decreases.

The existence of a correlation was tested on the mean values of the parameters at a significance level of 0.05. To that end, each calculated value of "*tau*" had to be equal to or greater (in absolute value) than the critical value defined in the reference Kendall table [41].

**Table 5**
Kendall correlation coefficient values for the assessment of relationships between shape indicators and properties of MK (Critical "*tau*" value at the 0.05 significance level = 1.00).

| | Calcination mode | Origin kaolinite | Water demand | BET $N_2$ | Cu | Cc |
|---|---|---|---|---|---|---|
| *Convexity* | | | | | | |
| [1–5[μm | 0.82 | 0.00 | 0.00 | 0.00 | −0.33 | −0.67 |
| [5–10[μm | 0.41 | 0.82 | **−1.00** | −0.67 | −0.33 | 0.00 |
| [10–15[μm | 0.00 | 0.82 | **−1.00** | −0.33 | −0.67 | −0.33 |
| [15–20[μm | 0.00 | 0.41 | −0.67 | 0.00 | **−1.00** | −0.67 |
| [20–40[μm | 0.41 | 0.00 | −0.67 | 0.33 | −0.67 | **−1.00** |
| >40 μm | 0.00 | 0.41 | −0.67 | 0.00 | **−1.00** | −0.67 |
| Mean* | 0.00 | 0.41 | −0.67 | 0.00 | **−1.00** | −0.67 |
| *Circularity* | | | | | | |
| [1–5[μm | 0.41 | 0.00 | −0.33 | 0.33 | −0.67 | **−1.00** |
| [5–10[μm | 0.00 | 0.82 | **−1.00** | −0.33 | −0.67 | −0.33 |
| [10–15[μm | 0.00 | 0.82 | **−1.00** | −0.33 | −0.67 | −0.33 |
| [15–20[μm | 0.00 | 0.41 | −0.67 | 0.00 | **−1.00** | −0.67 |
| [20–40[μm | 0.41 | 0.00 | −0.33 | 0.33 | −0.67 | **−1.00** |
| >40 μm | 0.00 | 0.41 | −0.67 | 0.00 | **−1.00** | −0.67 |
| Mean* | 0.00 | 0.41 | −0.67 | 0.00 | **−1.00** | −0.67 |
| *Elongation* | | | | | | |
| [1–5[μm | 0.00 | −0.82 | **1.00** | 0.33 | 0.67 | 0.33 |
| [5–10[μm | 0.00 | −0.82 | **1.00** | 0.33 | 0.67 | 0.33 |
| [10–15[μm | 0.00 | −0.82 | 0.67 | 0.00 | **1.00** | 0.67 |
| [15–20[μm | −0.41 | 0.00 | 0.33 | −0.33 | 0.67 | **1.00** |
| [20–40[μm | 0.00 | −0.41 | 0.67 | 0.00 | **1.00** | 0.67 |
| >40 μm | 0.00 | −0.41 | 0.67 | 0.00 | **1.00** | 0.67 |
| Mean* | 0.00 | −0.41 | 0.67 | 0.00 | **1.00** | 0.67 |

Significant relationships are in bold type.
* Mean value of all size classes from 1 μm.

*4.1. Relationships between morphology, origin, mode of calcination and resulting properties of metakaolin (fineness, water demand and size distribution)*

The Kendall "*tau*" values between the different parameters are presented in Table 5. The number *n* of pairs tested corresponds to the number of metakaolins. The critical value of "*tau*" is equal to 1.00. Several observations can be made.

- A strong correlation was observed between water demand and shape indicators: "*tau*" = 1 with elongation in [1–10[-μm classes and "*tau*" = −1 with convexity and circularity in [5–15[-μm classes. The main interpretation was found due to the existing amount of illite clay in MK1 and MK2 (Table 2) that accentuated the elongation of particles (Fig. 7c) as well as the water demand of the powder (Table 2).
- Although the relationships are not significant, convexity, circularity and elongation were linked to the origin of the kaolinite (impurity content of the raw material): "*tau*" = +0.82 with convexity and circularity in [5–15[-μm class and "*tau*" = −0.82 with elongation in [1–10[-μm class. Hence, a significant number of quartz grains, slightly or not at all modified by the calcination process, still existed in MK3 and MK4 (Table 2) and tended to produce more rounded and smoothed particles in some classes, depending on grinding intensity.
- Convexity of the finest particles ([1–5[-μm class) was only influenced by the calcination mode ("*tau*" = +0.82). The flash process could smooth the surface of the smallest particles.
- The BET specific surface was noticeably not correlated with any shape descriptor. This lack of correlation indicates open porosity, and it is likely that it also governs water demand. However, it is so fine that it cannot be fully accessible to the nitrogen molecules used to determine BET surface area. For this reason, there is a weak relationship between the BET surface area and the water demand ("*tau*" = +0.60).
- Depending on the size class, significant relationships or no relationships at all were observed between the uniformity and curvature coefficients and shape indicators (Table 5). However, there is no clear explanation for these observations. Instead, it appears more appropriate to discuss them in terms of a general trend. Indeed, in the experimental context, rounded, smooth particles belonged to metakaolins like MK4 presenting both narrow size distribution and a predominance of fine particles. Inversely, when circularity and convexity tended towards the lowest values (i.e., particles are more elongated and irregular), metakaolins exhibited spread size distribution, with MK1 and MK2 or without MK3 predominance of a particular size class.

At this stage, it is possible to conclude that the quantitative study on the morphology of metakaolin particles (Section 3.1.3) has not confirmed all the qualitative information obtained by SEM observations (Section 3.1.2). This can be explained by the fact that the notion of granulated particles is difficult to be admitted within metakaolin and a few SEM observations are not sufficient to objectively qualify morphological properties.

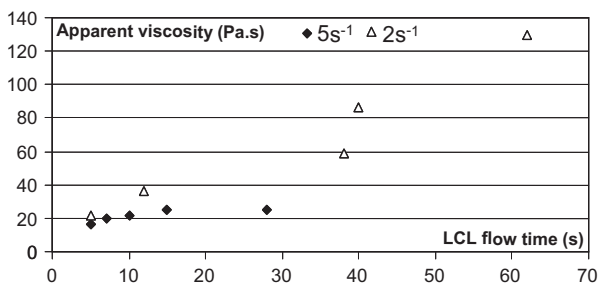


**Fig. 11.** Strong correlations between LCL flow time (5 min of age) and apparent viscosities at small shear rates for a given replacement level (12.5% or 25%).

*4.2. Relationships between size distribution, water demand, morphology of metakaolin and flow properties of mortars*

In this study, the number *n* of pairs tested corresponds to the number of powders, with the critical value of "*tau*" that is equal to 0.80. Before discussing the relationships between the properties of MK and the flow properties of mortars incorporating MK, the precise reasons for choosing some flow property values should be explained. The slump values at 5 min of age were considered because they discriminate better between the different mixes (Table 4). Although it is important to note that flow time (within 15 min of age for all suspensions) measured by the LCL workabilimeter can draw an image of the viscosity at small shear rates (perfect correlation ("*tau*" = 1) is given for 5 $s^{-1}$ at the 12.5% replacement level while it appears from 2 $s^{-1}$ at 25% replacement level, as shown in Fig. 11), there is more information provided by the measurement of the apparent viscosities at different shear rates. Accordingly, the influence of particle properties on viscosity can be discussed as a function of shear intensity.

In terms of the significant relationships between flow properties of mortars and properties of MK, several points should be mentioned.

- Although correlations were more marked at 25% replacement than 12.5% replacement, no significant correlations were found with the size distribution of powders (% passing less than 5 μm, $D_{10}$, $D_{50}$, $D_{90}$, Cu, Cc). Some trends show that flow properties can be influenced by the smallest sizes of the distribution (% passing less than 5 μm, $D_{10}$) and the extent of the size distribution (the more spread out the particle size distribution, the higher the viscosity). In any case, in an experimental context, describing MK fineness through size distribution (volume and number) is not sufficient to explain the variation in the flow of mortars.
- Conversely, the BET surface area is significantly related to (i) viscosity at low shear rates (2 $s^{-1}$ and 5 $s^{-1}$) for a 12.5% replacement level, and (ii) viscosity at any shear rate for a 25% replacement level (the greater the BET surface area, the higher the viscosity values). So, despite the fact that it does not represent the real surface of particles (Section 4.1), the $N_2$ BET surface area of powders (cement and MK) is a good indicator for predicting the flow of MK-based mixes.
- The water demand, depending on the open porosity of MK particles (Section 4.1), is significantly correlated to the flow properties of mortars when the replacement rate value is 25%: "*tau*" = −0.95 with slump and "*tau*" = +0.80 with viscosities at any shear rate studied. However, as already noted in Section 4.1, in addition to the intrinsic porosity of MK particles, the nature and the content of impurities can also act on water demand and morphology. For this reason, relationships between shape indicators and flow properties are expected. The most significant ones are provided in Table 6 and show us that circularity and convexity acted in the same way on slump and viscosities, which confirms that these indicators provide similar information.
- The signs of the significant correlations showed a logical evolution between parameters: when there was a decrease in slump and an increase in viscosity values, roundness and ruggedness of particles decreased and increased, respectively (with a decrease in circularity and convexity), and, obviously, elongation of particles increased. As the Kendall "*tau*" coefficient is sensitive to the rank of the paired observations between two

**Table 6**
Kendall correlation coefficient values for the assessment of relationships between flow properties and shape indicators.

| | Reference and 12.5% replacement level | | | | | Reference and 25% replacement level | | | |
|---|---|---|---|---|---|---|---|---|---|
| | Slump (5 min) | Visc2s$^{-1}$ | Visc5s$^{-1}$ | Visc15s$^{-1}$ | Visc25s$^{-1}$ | Slump (5 min) | Visc2s$^{-1}$ | Visc5s$^{-1}$ | Visc15s$^{-1}$ | Visc25s$^{-1}$ |
| *Convexity* | | | | | | | | | | |
| [1–5[μm | 0.00 | −0.40 | −0.60 | −0.40 | −0.40 | 0.53 | −0.60 | −0.60 | −0.60 | −0.60 |
| [5–10[μm | 0.40 | **−0.80** | **−1.00** | −0.40 | −0.40 | **0.95** | −1.00 | **−1.00** | **−1.00** | **−1.00** |
| [10–15[μm | 0.60 | −0.60 | **−0.80** | −0.60 | −0.60 | **0.95** | −0.80 | **−0.80** | **−0.80** | **−0.80** |
| [15–20[μm | 0.40 | −0.40 | −0.60 | **−0.80** | **−0.80** | 0.74 | −0.60 | −0.60 | −0.60 | −0.60 |
| [20–40[μm | 0.20 | −0.20 | −0.40 | **−0.80** | **−0.80** | 0.53 | −0.40 | −0.40 | −0.40 | −0.40 |
| >40 μm | 0.20 | −0.20 | −0.40 | **−1.00** | **−1.00** | 0.53 | −0.40 | −0.40 | −0.40 | −0.40 |
| Mean | 0.40 | −0.40 | −0.60 | **−0.80** | **−0.80** | 0.74 | −0.60 | −0.60 | −0.60 | −0.60 |
| *Circularity* | | | | | | | | | | |
| [1–5[μm | 0.20 | −0.20 | −0.40 | −0.60 | −0.60 | 0.53 | −0.40 | −0.40 | −0.40 | −0.40 |
| [5–10[μm | 0.60 | −0.60 | **−0.80** | −0.60 | −0.60 | **0.95** | **−0.80** | **−0.80** | **−0.80** | **−0.80** |
| [10–15[μm | 0.60 | −0.60 | **−0.80** | −0.60 | −0.60 | **0.95** | **−0.80** | **−0.80** | **−0.80** | **−0.80** |
| [15–20[μm | 0.40 | −0.40 | −0.60 | **−0.80** | **−0.80** | 0.74 | −0.60 | −0.60 | −0.60 | −0.60 |
| [20–40[μm | 0.20 | −0.20 | −0.40 | **−0.60** | **−0.80** | 0.53 | −0.40 | −0.40 | −0.40 | −0.40 |
| >40 μm | 0.20 | −0.20 | −0.40 | **−1.00** | **−1.00** | 0.53 | −0.40 | −0.40 | −0.40 | −0.40 |
| Mean | 0.40 | −0.40 | −0.60 | **−0.80** | **−0.80** | 0.74 | −0.60 | −0.60 | −0.60 | −0.60 |
| *Elongation* | | | | | | | | | | |
| [1–5[μm | −0.60 | 0.60 | **0.80** | 0.60 | 0.60 | **−0.95** | **0.80** | **0.80** | **0.80** | **0.80** |
| [5–10[μm | −0.60 | 0.60 | **0.80** | 0.60 | 0.60 | **−0.95** | **0.80** | **0.80** | **0.80** | **0.80** |
| [10–15[μm | −0.20 | 0.20 | 0.40 | **1.00** | **1.00** | −0.53 | 0.40 | 0.40 | 0.40 | 0.40 |
| [15–20[μm | 0.00 | 0.00 | 0.20 | **0.80** | **0.80** | −0.32 | 0.20 | 0.20 | 0.20 | 0.20 |
| [20–40[μm | −0.20 | 0.20 | 0.40 | **1.00** | **1.00** | −0.53 | 0.40 | 0.40 | 0.40 | 0.40 |
| >40 μm | −0.40 | 0.40 | 0.60 | **0.80** | **0.80** | −0.74 | 0.60 | 0.60 | 0.60 | 0.60 |
| Mean | −0.20 | 0.20 | 0.40 | **1.00** | **1.00** | −0.53 | 0.40 | 0.40 | 0.40 | 0.40 |

Critical "*tau*" value at the 0.05 significance level = 0.80. Significant relationships are in bold type.

tested properties, the expected relationships were found: M-0 and M-XMK4 mortars most often presented the highest flowability (Fig. 10) because cement and MK4 metakaolin incorporate more rounded and less elongated particles than other metakaolins (Fig. 7).

– The dependence of flow on morphology was marked in some size classes, especially in the case of higher replacement levels and higher influence of the finest classes (Table 6). Indeed, slump and viscosity at 2 s$^{-1}$ and 5 s$^{-1}$ were controlled by the shape of the smallest particles in a more marked way for the 25% replacement rate than for the 12.5% level. At higher shear rates (15 s$^{-1}$ and 25 s$^{-1}$), the viscosities of mortars incorporating MK at a replacement rate of 12.5% were influenced by the shape of particles larger than or equal to 10 μm, whereas they still depended on the morphology of particles smaller than 15 μm at a 25% replacement level. The increase in the amount of metakaolin induces an increase in the number of the finest particles. Hence, the number of larger particles becomes smaller in the suspension and the influence of such particles on viscosity becomes less significant.

**Table 7**
Illustrative example of data transformed into ranks (with ties).

| | Cement | MK1 | MK2 | MK3 | MK4 |
|---|---|---|---|---|---|
| *Convexity* | | | | | |
| [5–10[μm | 1 | 4 | 4 | 2 | 2 |
| [10–15[μm | 1 | 4 | 4 | 3 | 2 |
| *Circularity* | | | | | |
| [5–10[μm | 1 | 4 | 4 | 2 | 2 |
| [10–15[μm | 1 | 3 | 3 | 3 | 2 |
| *Elongation* | | | | | |
| [1–5[μm | 1 | 4 | 5 | 1 | 1 |
| [5–10[μm | 1 | 3 | 5 | 3 | 1 |
| *Slump* | | | | | |
| 5 min 12.5% | 1 | 4 | 4 | 3 | 1 |
| 5 min 25% | 1 | 5 | 4 | 3 | 2 |
| *Viscosity* | | | | | |
| 5s$^{-1}$ 12.5% | 1 | 2 | 5 | 2 | 2 |
| 5s$^{-1}$ 25% | 1 | 4 | 4 | 3 | 2 |
| Sum of ranks $R_i$ | 10 | 37 | 42 | 25 | 17 |

Ranking information: Convexity. Circularity and slump: from the highest (1) to the smallest (5).
Elongation and viscosity: from the smallest (1) to the highest (5).

In order to evaluate the degree to which the morphology of metakaolins and flow of mortars are in agreement with one another – and taking into account the results in Table 6, and the experimental scatter on each measured property – the data were transformed into ranks (with ties when there was no significant difference between the values of a given parameter measured on two powders or two mortars incorporating these powders). Accordingly, for a given property of powder/mortar, ranks were attributed for each powder (cement or MKi) and each mortar incorporating cement only or cement and MKi. An illustrative example is provided in Table 7. As a result, the determination of the tie-corrected value of the $W$ Kendall's coefficient of concordance is possible. Kendall's $W$ is a measure of the agreement among several $k$ measured properties (convexity, viscosity, etc.) that are assessing a given set of $n$ objects corresponding to the studied materials (powder or mortar) (Eq. (3)) [41].

$$W = \frac{12S}{k^2(n^3 - n) - k\sum_{j=1}^{k}\left[\sum_{a=1}^{s}(t_a^3 - t_a)\right]} \tag{3}$$

where $S = \sum_{i=1}^{n}(R_i - \bar{R})^2$ is a sum-of-squares statistic over the column sums of ranks $R_i$ ($\bar{R}$ is the mean of the $R_i$ values), $t_a$ = number of ties belonging to the set $a$ within the rank $j$.

The hypothesis of independence of the $k$ rankings was tested, and the calculated value of $W$ (taken from the data in Table 7) was equal to 0.89 and was mostly higher than the critical value of $W$ at the significance level of 0.05 (0.23). Hence, the classifications by the various parameters measured were not independent, and powders or mortars can be classified in the same order by whatever property was measured.

Finally, on the basis of the information in Table 7, it can be concluded that MK1, MK2 and, to a lesser extent, MK3, conferred the stiffest consistency and lowest flowability at low shear rates because they presented the least rounded, the most rugged and the most elongated particles in the fine classes ([1–20[ μm). Conversely, the reference mortar and mortars incorporating MK4 presented the finest consistency and lowest viscosity because cement and MK4 particles are the least elongated, rugged and the most rounded in the same size classes. This conclusion can be extended to the viscosities at high shear rates of mortars incorporating MK at a 25% replacement rate. At a 12.5% replacement level, the same result was maintained provided that size classes were shifted towards higher values (beyond 15 μm).

All of these results clearly show that it is possible to maintain or only minimally alter the flow properties of cement/metakaolin-based materials if metakaolin presents specific properties. In particular, the nature and content of impurities are key factors controlling the rheological properties of cementitious suspensions. They act directly on the morphology of the distribution of constituting particles and water demand; calcination mode seems to be a second order factor influencing the morphology of MK. The advantageous effect of MK4 on flowability measured at the mortar scale has been validated in real manufacturing conditions (slip forming concrete with 25% cement replacement by MK4 for precast beams and slabs) without any significant change in mechanical and durability aspects [42].

## 5. Conclusions

Properties of mortars incorporating four different metakaolins (MKi) were measured at the fresh state (slump, flow time, apparent viscosity at different shear rates). The mix proportion that was used per weight was 3:1:0.5 (sand:binder:water). The binder was composed of either 100% cement (OPC) or a combination of cement and MKi. Replacement rates of cement with MK were 12.5% and 25% per weight. The metakaolins were obtained through two different calcination processes (fluidised bed and flash) and were issued from two different extraction areas. Their chemical and mineralogical compositions, physical properties, size distribution and morphology were fully characterized. Despite the fact that they are referred to as "metakaolin," the results of this study show that calcined clays can produce significant differences in the flow of cement-based materials. The following conclusions have been supported by this research:

- Volume and number size distribution of MK particles are not sufficient to explain the variation in the flow properties depending on the nature of MK. However, BET surface area is a good indicator for predicting flow of MK-based mixes.
- Slump and viscosities are strongly dependent on the morphology of MK. When there is a decrease in slump and an increase in viscosity values, roundness and ruggedness of particles decrease and increase, respectively.
- The dependence of flow on morphology is marked in some size classes. Slump is controlled by the shape of the smallest particles at a 25% replacement rate. The influence of the size and shape of particles on viscosity is dependent on shear intensity. At low shear rates ($2\ s^{-1}$and $5\ s^{-1}$) and irrespective of the replacement rate, the smallest particles remain preponderant. At higher shear rates ($15\ s^{-1}$ and $25\ s^{-1}$), there is a predominance of particles larger or equal than 10 μm, provided that they are not diluted within the powder skeleton due to the increase in the replacement rate.
- The nature and content of impurities are the main parameters affecting the morphology of particles, and consequently, they affect the water demand of MK and the flow properties of the resulting mortars.
- High water demand is also dependent on an open porosity existing at the surface of the particles of both MK and impurities. However, a part of the porosity is so fine that it is not accessible to the nitrogen molecules used to measure the BET surface area. For this reason, a weak relationship was found between $N_2$ BET surface area and the water demand.
- The mode of calcination is a second order factor influencing the shape of particles. The flash process can smooth the surface of the smallest particles.
- This research has shown that an in-depth characterization of metakaolin is necessary before use in a concrete application. By studying the relationships between the properties of MK and the flow of cement/MK-based mortars, it can be definitively concluded that the water demand is not sufficient to categorize MK in relation to the flow properties of the whole mix. Indeed, although the water demand was always higher for any MK studied here than for cement, the high content of quartz present in flash MK as rounded particles was minimally or not at all affected by the calcination process, and maintained flow properties compared to those of mortar incorporating cement only. This effect has been validated in real manufacturing conditions (slip forming concrete with 25% cement replacement for precast beams and slabs) without any significant change in mechanical and durability aspects [40]. Accordingly, a metakaolin having significant water requirement and dilution generated by impurities like quartz can potentially be incorporated into cementitious materials.

## Acknowledgements

The authors are very grateful to SEAC-Gf enterprise and the Association Nationale de la Recherche Technique (ANRT) for supporting this research.

## References

[1] UNICEM. <http://www.unicem.fr> [Internet site of "UNICEM" 2012].
[2] Gartner E. Industrially interesting approaches to "low-$CO_2$" cement. Cem Concr Res 2004;34:1489–98.
[3] CIPEC. Canadian Industry Program for Energy Conservation. Energy consumption benchmark guide: cement clinker production, natural resources. Canada: Office of Energy Efficiency, M27–01-1464F; 2001.
[4] Kyoto Protocol. The United Nations framework convention on climate change, Kyoto Japan; 1990.
[5] Webmineral; 2011. <http://www.webmineral.com/data/Kaolinite.shtml>.
[6] Davies TW. Equipment for the study of flash heating of particles suspension. High Temp Technol 1984;3:141–7.
[7] Hénin JP, Pinoncely A. FCB et la calcination flash. Mines et Carrières Technologie 1986;6:249–52.
[8] Salvador S. Production de pouzzolanes de synthèse par calcinations flash de sols argileux: Etude des produits et conception d'une installation. PhD thesis. INSA Toulouse; 1992.
[9] Buathier S. Modélisation en régime dynamique d'un four tournant. DEA report of "Procédé, Systèmes, Matériaux" Université Paul Sabatier de Toulouse; 1998.
[10] Pera J. Metakaolin and calcined clay. Cement Concr Compos 2001;23:1.
[11] Cassagnabère F, Mouret M, Escadeillas G, Broilliard P, Bertrand A. Metakaolin, a solution for the precast industry to limit the clinker content in concrete: mechanical aspects. Construct Build Mater 2010;24:1109–18.
[12] Rojas MF, Cabrera J. Influence of MK on the reaction kinetics in MK/lime and water-blended cement systems at 20 C. Cem Concr Res 2001;31(4):519–27.
[13] Richardson IG. Tobermorite/jennite and tobermorite/calcium hydroxide based models for the structure of C–S–H: applicability to hardened pastes of tricalcium silicate, b-dicalcium silicate, Portland cement, and blends of Portland cement with blast-furnace slag, metakaolin or silica fume. Cem Concr Res 2004;34(9):1733–77.
[14] Cassagnabère F, Mouret M, Escadeillas G. Early hydration of clinker–slag–metakaolin combination in steam curing conditions, relation with mechanical properties. Cem Concr Res 2009;39(12):1164–73.
[15] Poon CS, Lam I, Kou SC, Wong YL, Wong R. Rate of pozzolanic reaction of metakaolin in high-performance cement pastes. Cem Concr Res 2001;31:1301–6.

[16] Brooks JJ, Megat Johari MA. Effect of metakaolin on creep and shrinkage of concrete. Cem Concr Compos 2001;23(6):495–502.
[17] Badogiannis E, Tsivilis S, Papadakis VG, Chaniotakis E. The effects of MK on concrete properties. In: Proceeding of Dundee conference, Dundee, UK; 2002. p. 81–9.
[18] Courard L, Darimont A, Schouterden M, Ferauche F, Willem X, Degeimbre R. Durability of mortar modified with metakaolin. Cem Concr Res 2003;33(9):1473–9.
[19] Gaboriau H, Gallias JL, Le Berre P. Utilisation des poudres minérales naturelles ultrafines pour l'amélioration des performances des bétons. In: Congrès de la Société de l'industrie Minérales, Montpellier, France; 1996.
[20] Wild S, Khatib JM, Jones A. Relative strength pozzolanic activity and cement hydration in superplasticized metakaolin concrete. Cem Concr Res 1996;26:1537–44.
[21] Bai J, Wild S, Ware JA, Sabir BB. Using neural networks to predict workability of concrete incorporating metakaolin and fly ash. Adv Eng Softw 2003;34:663–9.
[22] Li Z, Ding Z. Property improvement of Portland cement by incorporating with metakaolin and slag. Cem Concr Res 2003;33:579–84.
[23] European Standard Institution. Methods of testing cement. Determination of setting time and soundness. European Standard Institution; 2005 [NF EN196-3].
[24] Badogiannis E, Kakali G, Dimopoulou G, Chaniotakis E, Tsivilis S. Metakaolin as a main cement constituent. Exploitation of poor Greek kaolin's. Cem Concr Compos 2005;27(2):197–203.
[25] European Standard Institution. Cement – Part 1: composition, specifications and conformity criteria for common cements. European Standard Institution; 2000 [NF EN197-1].
[26] European Standard Institution. Methods of testing cement. Determination of strength. European Standard Institution; 2006 [NF EN196-1].
[27] Cassagnabère F. Precast elements in slip forming concrete: from the improvement of the material to better management of the manufactured process. PhD thesis of Université de Toulouse; 2007.
[28] Sedran T. Rhéologie et rhéomètrie des bétons: application aux bétons autonivelants. PhD thesis ENPC de Paris; 1999.
[29] Legrand C. A contribution to the study of fresh concrete rheology. Mater Construct 1972;29:275–95.
[30] Metzner AB. Rheology of suspensions in polymeric liquids. J Rheol 1985;29(6):739–75.
[31] Luerkens DW. Theory and applications of morphological analysis: fine particles and surface. London: CRC Press; 1991.
[32] Hentschel ML, Page NW. Selection of descriptors for particle shape characterization. Particle Particle Syst Character. 2003;20:25–38.
[33] Schartzentruber A, Catherine C. La méthode du Mortier de Béton Equivalent (MBE): Un nouvel outil d'aide à la formulation de bétons adjuvantés. Mater Struct 2000;33(8):475–82.
[34] French standard institution. measuring the flow time of concrete and mortar using a workability meter. French Standard Institution; 1988 [NF P18-452].
[35] Garcia-Diaz E. Réactivité pouzzolanique des metakaolinites: corrélations avec les caractéristiques mineralo-gitologiques des kaolinites. PhD thesis. Ecoles des Mines de St Etienne; 1995.
[36] Shapiro SS, Wilk MB. An analysis of variance test for normality (complete samples). Biometrika 1965;52(3–4):591–611.
[37] Johnson RW. An introduction to the Bootstrap. Teaching Stat 2001;23(2):49–54.
[38] Saak AW, Jennings HM, Shah SP. A generalized approach for the determination of yield stress by slump and slump flow. Cem Concr Res 2004;34(3):363–71.
[39] Cyr M, Legrand C, Mouret M. Study of the shear thickening effect of superplasticizers on the rheological behaviour of cement pastes containing or not mineral additives. Cem Concr Res 2000;30:1477–83.
[40] Reed JS. Principles of ceramic processing. 2nd ed. New York: John Wiley and Sons; 1995.
[41] Sheskin DJ. Handbook of parametric and nonparametric statistical procedures. 3rd ed. Chapman & Hall/CRC; 2004.
[42] Cassagnabère F, Mouret M, Escadeillas G, Broilliard P. Use of flash metakaolin in a slip-forming concrete for precast industry. Magaz Concr Res 2008;61(10):767–78.